

# BIOSYNTHESIS OF SILVER NANOPARTICLES FROM SENNA AURICULATA AND SYMPLOCOS RACEMOSA FORMULATION AND ITS ANTIMICROBIAL MECHANISM OF ACTION AGAINST WOUND PATHOGENS

PRASHEETHA S<sup>A</sup>, DINESH KUMAR<sup>B</sup>, DHANYAA MUTHUKUMARAN<sup>A</sup>, RAJESHKUMAR SHANMUGAM<sup>A</sup>

<sup>A</sup>NANOBIOMEDICINE LAB, DEPARTMENT OF ANATOMY, SAVEETHA MEDICAL COLLEGE AND HOSPITAL, SAVEETHA INSTITUTE OF MEDICAL AND TECHNICAL SCIENCES (SIMATS), CHENNAI, TAMIL NADU, INDIA.

<sup>B</sup>DEPARTMENT OF COMMUNITY MEDICINE, SAVEETHA MEDICAL COLLEGE AND HOSPITAL, SAVEETHA INSTITUTE OF MEDICAL AND TECHNICAL SCIENCES (SIMATS), CHENNAI, TAMIL NADU, INDIA

## Abstract

**Aim:** To synthesize silver nanoparticles (AgNPs) using *Senna auriculata* and *Symplocos racemosa* extracts and evaluate their antimicrobial and antibiofilm activities against wound-associated bacterial pathogens.

**Introduction:** In this study, *S. auriculata* and *S. racemosa* were selected as plant sources for the eco-friendly, green synthesis of AgNPs, leveraging their known ethnopharmacological properties. Wound infections are often caused by antibiotic-resistant pathogens such as *Pseudomonas* sp., *Actinobacter* sp., *Enterococcus faecalis*, *Escherichia coli*, and *Staphylococcus aureus*, leading to delayed healing and increased morbidity. Silver nanoparticles have emerged as effective antimicrobial agents due to their broad-spectrum activity and ability to disrupt biofilms. Green synthesis using medicinal plants offers an eco-friendly, cost-effective route to nanoparticle production, combining phytochemicals with nanotechnology for enhanced therapeutic outcomes.

**Methods:** The visual confirmation by a color change and spectroscopically validated via UV-Vis absorption at 450 nm. Using an agar well diffusion assay, the AgNPs at different concentrations were tested against wound pathogens, and the inhibition zones were measured to determine antibacterial efficacy. For the Time-Kill Kinetics Assay, the bactericidal effect of AgNPs was analyzed over 5 hours using optical density and CFU counts to assess the time- and dose-dependent killing pattern at varying concentrations. For the Antibiofilm Assay, Mature biofilms of each pathogen were treated with AgNPs (25–100 µg/mL), and biofilm mass was quantified using ELISA at 590 nm after PBS washing and scraping.

**Results:** AgNPs showed excellent antimicrobial activity, with the largest zone of inhibition (13 mm × 10 mm) against *Actinobacter* sp. at 100 µg/mL, followed by *Pseudomonas* sp. and *S. aureus*. The time-kill assay revealed that 100 µg/mL of AgNP nanofilm significantly reduced viable bacterial counts within 3–4 hours, particularly in *E. coli* and *S. aureus*. Antibiofilm activity was also dose-dependent, with *Actinobacter* sp. biofilms exhibiting the highest sensitivity, followed by *S. aureus* and *Pseudomonas* sp.

**Conclusion:** The green-synthesized AgNPs from *S. auriculata* and *S. racemosa* demonstrated potent antimicrobial and antibiofilm effects against key wound pathogens. Their incorporation into polymeric nanofilms enhances sustained antimicrobial action, supporting their potential use in advanced wound dressings. These findings offer a promising, eco-friendly alternative for infection control and wound management in the context of rising antibiotic resistance.

**Keywords:** Silver nanoparticles, *Senna auriculata*, *Symplocos racemosa*, Antibacterial activity, Wound pathogens, Nanofilms.

## INTRODUCTION

Nanobiotechnology is a rapidly evolving interdisciplinary field that bridges biology and nanotechnology, focusing on the design and development of nanoscale materials for biomedical and environmental applications.

(1) One of the central components in this domain is the use of nanoparticles (NPs), which are materials sized between 1 and 100 nanometers that exhibit unique physical, chemical, and biological characteristics due to their high surface-area-to-volume ratio. (2,3)

Among various methods of nanoparticle synthesis, green synthesis has gained considerable attention due to its eco-friendliness, cost-effectiveness, and biocompatibility. (4) This method uses biological agents such as plant extracts, bacteria, fungi, or algae to reduce metal ions into nanoparticles without involving harmful chemicals. (5,6) The bioactive compounds in plant extracts act as both reducing and stabilizing agents, enabling the production of stable and functionally active nanoparticles. (7)

Green-synthesized nanoparticles are widely explored for their antimicrobial, antioxidant, anti-inflammatory, and wound-healing properties. (8,9) Silver nanoparticles (AgNPs), in particular, are one of the most studied nanomaterials due to their broad-spectrum antimicrobial efficacy, ability to generate reactive oxygen species, and strong interaction with microbial membranes and proteins. (10,11)

*S. auriculata*, commonly known as Tanner's Cassia, is a medicinal plant native to India. Its flowers are rich in phenolic compounds, flavonoids, alkaloids, and saponins, which contribute to its antioxidant, antimicrobial, and anti-inflammatory activities. (12,13) Studies have shown that *S. auriculata* extracts can inhibit the growth of wound-associated pathogens (14,15)

*S. racemosa*, another ethnomedicinal plant, has been traditionally used for treating inflammation and microbial infections. The bark of this plant contains tannins, flavonoids, glycosides, and alkaloids, which are known for their antimicrobial potential. (16,17) Extracts of *S. racemosa* have demonstrated activity against multiple wound pathogens. (18)

AgNPs synthesized using plant extracts exhibit enhanced bioactivity due to the synergistic action of silver and phytochemicals. (19) These nanoparticles are known for their excellent wound healing capabilities due to their antibacterial, antioxidant, and anti-inflammatory effects, making them suitable for topical therapeutic applications. (20,21) Recent advances have enabled the development of nanofilms incorporating AgNPs for controlled drug release and localized therapy in wound care. (22)

Wound infections caused by microbial pathogens are a significant healthcare challenge worldwide, often leading to delayed healing, chronic wounds, and increased morbidity. (23,24) Common wound pathogens include *Pseudomonas sp.*, *Actinobacter sp.*, *Enterococcus faecalis*, *Escherichia coli*, and *Staphylococcus aureus*, which are known for their ability to form biofilms that confer resistance to antibiotics and the host immune response. (3,4) These biofilms hinder wound healing by protecting bacteria from antimicrobial agents and contributing to persistent infections. (5,6)

The rise of antibiotic-resistant strains among these pathogens exacerbates the problem, limiting treatment options and increasing healthcare costs. (7) Therefore, developing novel, effective antimicrobial agents that can overcome biofilm resistance is critical for improving wound management. (8)

Silver nanofilms, composed of polymer matrices loaded with AgNPs, serve as protective antimicrobial barriers that can prevent infection and promote healing by maintaining a moist wound environment and releasing nanoparticles over time. (23) These films are ideal for treating chronic wounds, diabetic ulcers, and burns due to their sustained activity and biocompatibility. (24)

This study aims to biosynthesize silver nanoparticles using flower extracts of *S. auriculata* and bark extracts of *S. racemosa*, fabricate them into a nanofilm, and investigate their antimicrobial activity against common wound pathogens. This research seeks to provide an effective, plant-based alternative for antimicrobial wound therapy.

## MATERIALS AND METHODS

### Preparation of *S.auriculata* flower and *S.racemosa* bark extract

0.25g of *S.auriculata* and *S.racemosa* was weighed and added to 50ml of distilled water [Fig. (a)] and heated for 15 -20min at 50°C using a heating mantle [Fig. (b)]. It was then filtered using a muslin cloth [Fig. (c)] and the plant filtrate was collected [Fig. (d)].

### Preparation of Silver nitrate solution:

2mM of silver nitrate was weighed and was mixed with 80mL of distilled water [Fig1(e)]

### Preparation of *S. auriculata* + *S. racemosa* - Ag NPs

20mL of the filtered extract was then mixed with 80mL of silver nitrate solution [Fig1(h)] After 24 hours the colour change was observed. After 48 hours, the nanoparticle solution was centrifuged at 8000 rpm for 10 minutes. The pellet was collected. [Fig1(j)]

### Preparation of Ag nanofilm:

0.5g of PVA (Poly vinyl alcohol) in 10 ml of distilled water and 0.1g of Chitosan in 10mL of distilled water was prepared, and 1 ml of *S.auriculata*+*S.racemosa*-Ag NPs were mixed well using a magnetic stirrer for 24 hrs, then 5ml of the obtained product was kept in a Hot air oven until the film was formed. [Fig1(i)]

### Antimicrobial activity:

#### Agar well diffusion method

The antimicrobial activity of the green synthesized silver nanoparticles was evaluated using the agar well diffusion technique. Mueller Hinton agar plates were prepared and sterilized using an autoclave at 121°C for 15-20 minutes. After sterilization, the medium was poured onto the surface of sterile Petri plates and allowed to cool to room temperature. The bacterial culture (*Pseudomonas sp.*, *Actinobacter sp.*, *E. faecalis*, *E. coli*, *S. aureus*) was spread evenly onto the agar plates using sterile cotton swabs. Wells of 9 mm diameter were created in the agar plates using a sterile polystyrene tip. The wells were then filled with different concentrations (25, 50, 100 µg/mL) of AgNPs. An antibiotic (e.g., bacteria - Amoxicillin, Fungi-Fluconazole) was used as a standard. The plates were incubated at 37°C for 24 hours and 48 hours for fungal cultures.

#### Time kill kinetics:

A time-kill curve assay was conducted to assess the bactericidal properties and concentration-dependent relationship between *S. auriculata* and *S. racemosa*-mediated silver nanoparticles and the net growth rate of *Pseudomonas sp.*, *Actinobacter sp.*, *E. faecalis*, *E. coli*, and *S. aureus* over regular time intervals. The assay involved culturing the three wound pathogens in Mueller-Hinton Broth supplemented with varying concentrations of silver nanoparticles (25, 50, and 100 µg/ml), followed by time-kill curve analysis. An antibiotic (e.g., Bacteria - amoxicillin, Fungi-Fluconazole) was used as a standard. After a pre-incubation period of four hours in a medium devoid of any antimicrobial agents, growth curves were carried out before the test to ensure that all pathogens had reached a stable early-to-mid log phase. An inoculum consisting of 0.5 McFarland of each pathogen was created in sterile phosphate-buffered saline. This inoculum was collected from cultures that had been cultivated on Mueller-Hinton agar plates at 37°C for 18–20 h. After that, 30 µL of the inoculum was diluted in 15 mL of antimicrobial-free Mueller-Hinton Broth medium that had been pre-heated to 37 °C, and 90 µL The resultant mixture was distributed evenly over each well of a 96-well ELISA plate. To each well containing 90 µL of pre-incubated wound pathogens, 10 µL of *S. auriculata* and *S. racemosa*-mediated silver nanoparticles at five different concentrations was added, along with the untreated control.

#### Antibiofilm Assay

The antibiofilm assay encompassed the assessment of biofilm eradication efficacy, following a methodology reported by Sasarom et al. in their research in 2023. Initially, biofilms were permitted to mature within a 96-well microtiter plate, following established protocols, over a 72-hour incubation period. Subsequent to incubation, the culture medium was withdrawn, and the wells were rinsed thrice with PBS phosphate-buffered saline to eliminate non-adherent cells. Following this, 300 µL of Ag nanoparticle (NP) solutions were introduced into the wells. After a specified duration, the AgNP solutions were discarded, and the biofilms adhering to the plates were subjected to a triple PBS wash. The biofilms were meticulously scraped and homogenized, and the resulting samples were subjected to serial dilution in PBS. These dilutions were subsequently assessed using an ELISA reader, with measurements taken at 590 nm.

## RESULTS

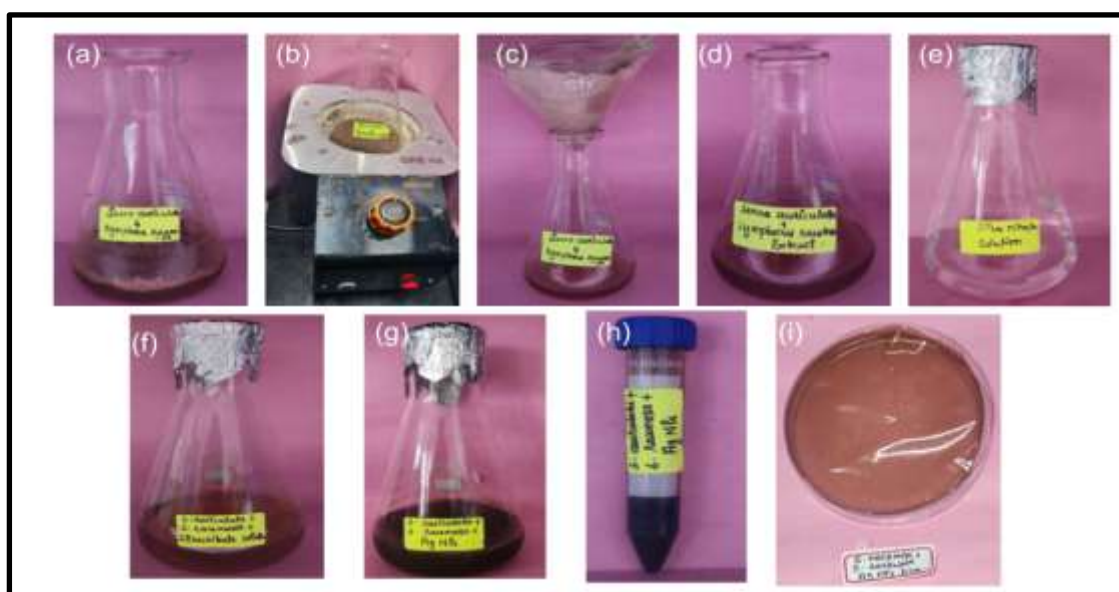


**Fig 1:** Visual representation of Preparation and synthesis of the herbal formulation of *S. auriculata* *S. racemosa* -Ag NPs mediated nanofilm

### Visual observation:

The change in colour from light brown to dark brown after 48 hours confirms the synthesis of AgNPs.[Fig1(g)]

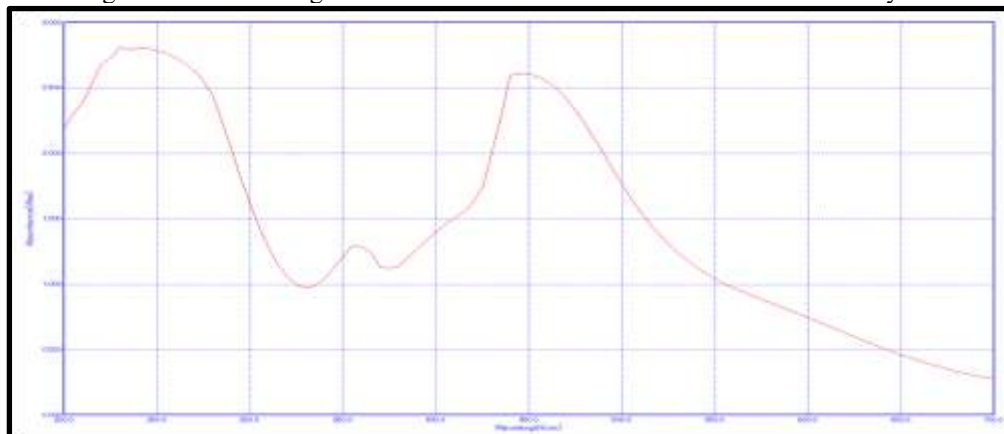


**Fig 2:** Graphical representation of UV visual spectroscopy of *S. auriculata* and *S. racemosa* formulation- AgNPs

The synthesis of silver nanoparticles (Ag-NPs) was confirmed through UV-Visible spectrophotometric analysis. The absorption spectrum displayed a prominent peak at 445 nm, which corresponds to the surface plasmon resonance (SPR) characteristic of silver nanoparticles.

### Antimicrobial activity:

#### Agar well diffusion method:

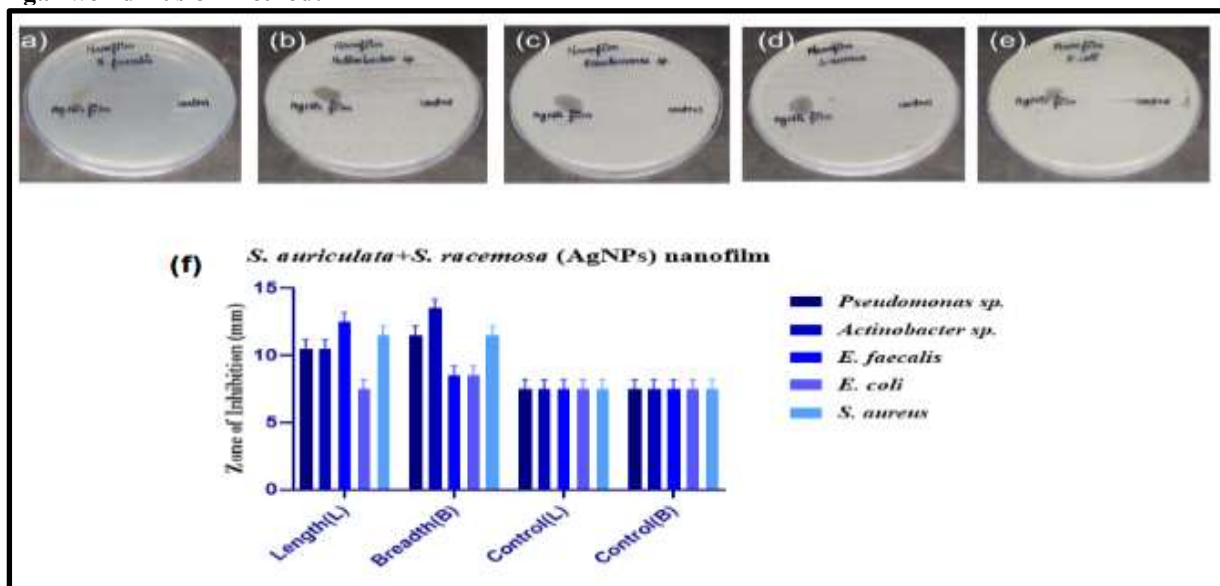


**Fig 3:** Agar well diffusion images of *S. auriculata* and *S. racemosa* formulation-mediated AgNPs a) *E. faecalis* b) *Actinobacter sp.* c) *Pseudomonas sp* d) *S. aureus* e) *E. coli*

(f) Graphical representation of antimicrobial activity by agar well diffusion method using *S. auriculata* and *S. racemosa* formulation- AgNPs nanofilm

The antimicrobial potential of the synthesized silver nanoparticles (AgNPs) was evaluated in (Fig 3a-e) using the agar well diffusion method against wound pathogens, including *Pseudomonas sp.*, *Actinobacter sp.*, *E. faecalis*, *E. coli*, and *S. aureus*. The inhibition zones increased with the presence of Ag NPs, with the highest inhibition in measurements of 11 mm in length and 12 mm in breadth in *Pseudomonas sp* followed by 10mm in length and 13 mm in breadth in *Actinobacter sp.*, and with the measurements of 12mm in length and 8mm in breadth in *E. faecalis* and with the measurements 11 mm in length and 11mm in breadth in *S.aureus* and with the measurements of 7mm in length and 8mm in breadth in *E.coli* was noted. These measurements were compared with the control, where there was no zone of inhibition observed.



### Time-Kill Kinetic Analysis:

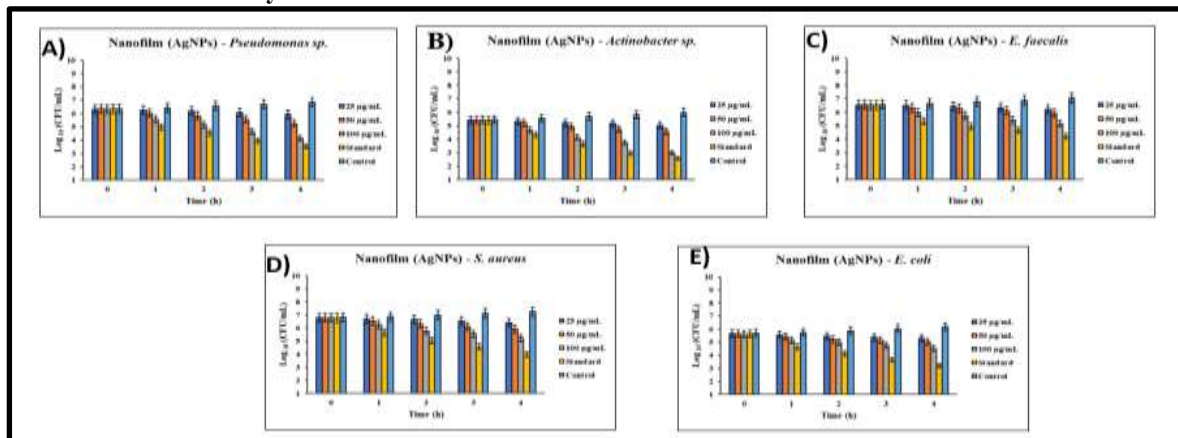


**Fig 4:**Graphical representation of Time kill kinetics assay using *S. auriculata* and *S. racemosa* mediate AgNPs  
a) *Pseudomonas sp.*, b) *Actinobacter sp.*, c) *E. faecalis*, d) *S. aureus*, e) *E. coli*

The bacteriostatic and bactericidal activities of AgNP nanofilms were evaluated against five bacterial strains: *Pseudomonas sp.*, *Actinobacter sp.*, *E. faecalis*, *S. aureus*, and *E. coli* over 5 hours at various concentrations (25, 50, 100  $\mu\text{g/mL}$ ).

The data demonstrate a dose- and time-dependent antimicrobial effect across all strains. Notably, at a higher concentration (100  $\mu\text{g/mL}$ ) of AgNPs nanofilms, significant bactericidal activity was observed, particularly after 3–4 hours. For instance, in *E. coli* (fig. 4 E), the 100  $\mu\text{g/mL}$  treatment reduced bacterial load to nearly undetectable levels by hour 4, indicating strong bactericidal effects.

At lower concentrations (25 and 50  $\mu\text{g/mL}$ ), the nanofilms primarily exhibited bacteriostatic activity, as evidenced by inhibition of bacterial growth without a drastic reduction compared to the control. This was especially apparent in *Actinobacter sp.* and *E. faecalis* (fig.B and C), where bacterial counts remained stable or slightly decreased over time under lower doses.

Among all tested strains, *S. aureus* (fig.D) and *E. coli* (fig. E) were the most susceptible to AgNPs nanofilms, indicating a pronounced bactericidal response. In contrast, *Pseudomonas sp.* (fig.A) demonstrated relatively higher resistance, requiring higher AgNPs concentrations to achieve comparable bactericidal effects.

These findings suggest that AgNPs nanofilms can effectively exert both bacteriostatic and bactericidal activity, depending on the concentration and exposure time, supporting their potential use in antimicrobial coatings or wound dressings.

### Antibiofilm activity:

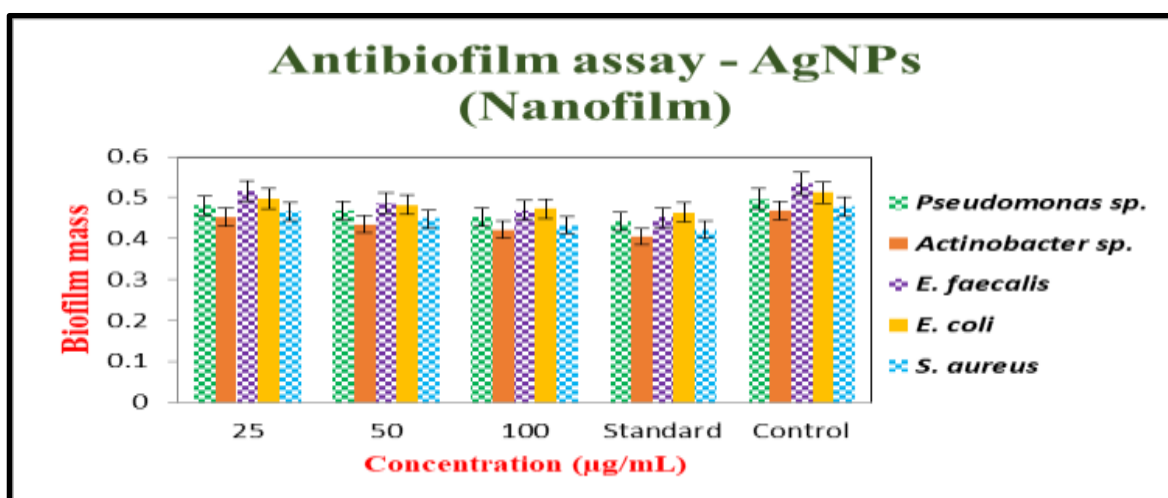


**Fig. 5:** Graphical representation of antibiofilm assay using *S. auriculata* and *S. racemosa* formulation-mediated AgNPs

Antibiofilm activity of *S. auriculata* and *S. racemosa* formulation-mediated AgNPs was assessed using anti-biofilm assay, which evaluates the ability to inhibit the formation of microbial biofilms of *Pseudomonas sp.*, *Actinobacter sp.*, *E. faecalis*, *E. coli*, and *S. aureus*, revealing a dose-dependent enhancement in antibacterial activity. From the study, the biosynthesis of *S. auriculata* and *S. racemosa* formulation-mediated AgNPs shows similar results at a higher concentration of 100 µg/mL when compared to the standard. At 100µg/mL, the *Actinobacter sp.* shows the highest inhibition, followed by *S. aureus*, *Pseudomonas sp.*, *E. faecalis*, and *E. coli*. At 50µg/mL the *Actinobacter sp.* shows the highest inhibition, followed by *S. aureus*, *Pseudomonas s.*, *E. coli*, and *E. faecalis*. At 25µg/mL, the *Actinobacter sp.* shows the highest inhibition, followed by *S. aureus*, *Pseudomonas s.*, *E. coli*, and *E. faecalis*. These values show that at a higher concentration, the AgNPs show a significant antibacterial activity.

## DISCUSSION

The current study demonstrates the successful green synthesis of AgNPs using the aqueous flower extract of *S. auriculata* and bark extract of *S. racemosa*, as indicated by the visual color change from light brown to dark brown, and further confirmed by UV-Visible spectrophotometry, which showed a distinct peak at 450 nm. This surface plasmon resonance is characteristic of AgNPs and aligns with observations reported where Ginger-mediated AgNPs exhibited an absorption peak near 450 nm, confirming nanoparticle formation through plant-mediated reduction of Ag<sup>+</sup> ions [29].

The antimicrobial activity of the synthesized AgNPs was evaluated against five wound pathogens — *Pseudomonas sp.*, *Actinobacter sp.*, *E. faecalis*, *S. aureus*, and *E. coli*. The agar well diffusion assay showed that the AgNPs had significant inhibitory effects, with the largest zones of inhibition recorded for *Actinobacter sp.* (13 mm × 10 mm) and *Pseudomonas sp.* (12 mm × 11 mm) at 100 µg/mL concentration. against *Pseudomonas sp.* and *S. aureus* using *Senna auriculata*-derived AgNPs [25,26,27]. Moreover, Nandhini et al. (2023) found comparable results using *Symplocos racemosa* leaf-mediated AgNPs against *E. faecalis*, achieving inhibition zones ranging from 8 to 11 mm depending on concentration [1].

Time-kill kinetic assays confirmed a concentration- and time-dependent bactericidal effect of the nanofilm-embedded AgNPs. At 100 µg/mL, a significant reduction in bacterial viability was observed within 3–4 hours, especially in *E. coli* and *S. aureus*, where colony-forming units (CFUs) dropped to near-undetectable levels. They demonstrated that silver nanoparticles caused complete bacterial kill in *E. coli* within 4 hours at 100 µg/mL, with a similar decline in *S. aureus* viability. In contrast, *Pseudomonas sp.* exhibited relatively higher resistance, requiring prolonged exposure or higher doses for significant CFU reduction, who reported that *P. aeruginosa* biofilms showed delayed sensitivity to AgNPs compared to planktonic forms [26].

The antibiofilm activity further emphasized the potential of AgNPs in treating chronic wounds. At 100 µg/mL, *Actinobacter sp.* biofilms were most effectively disrupted, followed by those of *S. aureus*, *Pseudomonas sp.*, and *E. faecalis*. The reduction in biofilm biomass was significant when compared to the untreated control, and closely matched the inhibition levels produced by standard antibiotics. Spireseu et al. (2021) also reported strong antibiofilm properties of green-synthesized AgNPs, particularly against Gram-positive pathogens such as *S. aureus* and *E. faecalis*, where they reduced biofilm mass by more than 60% at similar concentrations [28,29]. This suggests that the combination of bioactive phytochemicals and AgNPs provides a synergistic effect, enhancing antimicrobial efficacy, particularly in disrupting the protective extracellular polymeric substance (EPS) layer of biofilms.

When compared with other AgNPs-based nanofilms, the current study's results are consistent in demonstrating strong antimicrobial action, reported zones of inhibition between 12–16 mm using AgNP-loaded wound dressings, similar to the 13 mm observed here against *Actinobacter sp.* Likewise, observed >70% biofilm disruption and rapid bacterial reduction within 4 hours, respectively, outcomes closely matching our time-kill and antibiofilm results. However, as Sousa et al. [45] highlighted, higher AgNP concentrations may pose pro-inflammatory risks, emphasizing the importance of careful dosage design for biomedical applications.[30]

## CONCLUSION

This study successfully demonstrated the green synthesis of silver nanoparticles using *S. auriculata* flower and *S. racemosa* bark extracts, confirming their potent antimicrobial and antibiofilm activities against key wound pathogens. Synthesized AgNPs exhibited concentration-dependent bacteriostatic and bactericidal effects. The integration of phytochemicals from these plants enhanced nanoparticle stability and biological efficacy. These findings highlight the potential of plant-mediated AgNPs as effective, eco-friendly alternatives for antimicrobial wound dressings and coatings, addressing challenges of antibiotic resistance and chronic wound infections. Future work should include in vivo assessments and cytotoxicity evaluations to advance clinical applications.

## REFERENCES

1. Nandhini SN, Sisubalan N, Vijayan A, Karthikeyan C, Gnanaraj M, Gideon DA, Jebastin T, Varaprasad K, Sadiku R. Recent advances in green synthesized nanoparticles for bactericidal and wound healing applications. *Heliyon*. 2023 Feb 1;9(2):e12699.
2. Nqakala ZB, Sibuyi NR, Fadaka AO, Meyer M, Onani MO, Madiehe AM. Advances in nanotechnology towards development of silver nanoparticle-based wound-healing agents. *Int J Mol Sci*. 2021;22(20):11272.
3. Kiarashi M, Mahamed P, Ghotbi N, Tadayonfard A, Nasiri K, Kazemi P, Badkoobeh A, Yasamineh S, Joudaki A. Spotlight on therapeutic efficiency of green synthesis metals and their oxide nanoparticles in periodontitis. *J Nanobiotechnol*. 2024;22(1):21.
4. Dhaka A, Mali SC, Sharma S, Trivedi R. A review on biological synthesis of silver nanoparticles and their potential applications. *Results Chem*. 2023;6:101108.
5. Singh S, Tiwari H, Verma A, Gupta P, Chattopadhyaya A, Singh A, Singh S, Kumar B, Mandal A, Kumar R, Yadav AK. Sustainable synthesis of novel green-based nanoparticles for therapeutic interventions and environmental remediation. *ACS Synth Biol*. 2024;13(7):1994-2007.
6. Menichetti A, Mavridi-Printezi A, Mordini D, Montalti M. Effect of size, shape and surface functionalization on the antibacterial activity of silver nanoparticles. *J Funct Biomater*. 2023;14(5):244.
7. Rodrigues AS, Batista JG, Rodrigues MÁ, Thipe VC, Minarini LA, Lopes PS, Lugão AB. Advances in silver nanoparticles: a comprehensive review on their potential as antimicrobial agents and their mechanisms of action elucidated by proteomics. *Front Microbiol*. 2024;15:1440065.
8. Ansari MA. Nanotechnology in food and plant science: challenges and future prospects. *Plants*. 2023;12(13):2565.
9. Lo S, Mahmoudi E, Fauzi MB. Applications of drug delivery systems, organic, and inorganic nanomaterials in wound healing. *Discover Nano*. 2023;18(1):104.
10. Shalaby MA, Anwar MM, Saeed H. Nanomaterials for application in wound healing: Current state-of-the-art and future perspectives. *J Polym Res*. 2022;29(3):91.
11. Laganà A, Visalli G, Corpina F, Ferlazzo M, Di Pietro A, Facciola A. Antibacterial activity of nanoparticles and nanomaterials: a possible weapon in the fight against healthcare-associated infections. *Eur Rev Med Pharmacol Sci*. 2023;27(8).
12. Sabarees G, Velmurugan V, Tamilarasi GP, Alagarsamy V, Raja Solomon V. Recent advances in silver nanoparticles containing nanofibers for chronic wound management. *Polymers*. 2022;14(19):3994.
13. Pechyen C, Tangnorawich B, Toommee S, Marks R, Parcharoen Y. Green synthesis of metal nanoparticles, characterization, and biosensing applications. *Sensors Int*. 2024;100287.
14. Anvar AA, Ahari H, Ataee M. Antimicrobial properties of food nanopackaging: A new focus on foodborne pathogens. *Front Microbiol*. 2021;12:690706.
15. Chaudhary J, Tailor G, Yadav M, Mehta C. Green route synthesis of metallic nanoparticles using various herbal extracts: A review. *Biocatal Agric Biotechnol*. 2023;50:102692.
16. Ghosh S, Roy S, Naskar J, Kole RK. Plant-mediated synthesis of mono- and bimetallic (Au–Ag) nanoparticles: Future prospects for food quality and safety. *J Nanomater*. 2023;2023:2781667.
17. Dash KK, Deka P, Bangar SP, Chaudhary V, Trif M, Rusu A. Applications of inorganic nanoparticles in food packaging: A comprehensive review. *Polymers*. 2022;14(3):521.
18. Danai L, Rolband LA, Perdomo VA, Skelly E, Kim T, Afonin KA. Optical, structural and antibacterial properties of silver nanoparticles and DNA-templated silver nanoclusters. *Nanomedicine*. 2023;18(9):769–82.
19. Ren R, Lim C, Li S, Wang Y, Song J, Lin TW, Muir BW, Hsu HY, Shen HH. Recent advances in the development of lipid-, metal-, carbon-, and polymer-based nanomaterials for antibacterial applications. *Nanomaterials*. 2022;12(21):3855.
20. Kumar V, Kumar N. Therapeutic Effect of Herbal Medicinal Plants on Polycystic Ovarian Syndrome: A Review. *Asian J Pharm Res Dev*. 2022;10(6):153–60.
21. Kumar GS, Garg K, Soni A, Dalal M. A Comprehensive Review of Preclinical Models for Polycystic Ovary Syndrome. *Curr Drug Ther*. 2024;19(4):426–37.
22. Tiwari S, Singh S. A comprehensive review of acne's facial impact and the therapeutic potential of Indian herbal medicine. *World J Adv Res Rev*. 2024;23(3):1148–55.
23. Liaqat A, Mallhi TH, Khan YH, Khokhar A, Chaman S, Ali M. Anti-snake venom properties of medicinal plants: a comprehensive systematic review of literature. *Braz J Pharm Sci*. 2022;58:e191124.
24. Cherian S, Karthega M. In Vitro Studies on Bioactive *Senna Auriculata* Flower Extract Incorporated PCL-Cellulose Acetate Electrospun Nanofiber for Wound Dressing Application. *SSRN*. Available from: <https://ssrn.com/abstract=5152362>

25. Shanmuga, S. S., Mariraj, I., Rajeshkumar, S., Dhanyaa, M., & Pradeep, M. (2025). In vitro biological evaluation of silver nanoparticles synthesized using zingiber officinale and ocimum gratissimum herbal formulation. *The Medical journal of Malaysia*, 80(Suppl 1), 20–25.
26. GIRIPRASAD M, YASHVANTHAN VR, SHANMUGAM R, MUTHUKUMARAN D, ABARNA DJ. EVALUATION OF ANTIBACTERIAL AND TIME-KILL KINETICS ANALYSIS OF ASPALATHUS LINEARIS MEDIATED SELENIUM NANOPARTICLES AGAINST STREPTOCOCCUS MUTANS AND STAPHYLOCOCCUS AUREUS. TPM [Internet]. 2025 Aug. 11 [cited 2025 Sep. 3];32(S2(2025) : Posted 09 June):286-93. Available from: <https://tpmap.org/submission/index.php/tpm/article/view/227>
27. Anishya D, Jain RK. Vanillin-Mediated Green-Synthesised Silver Nanoparticles' Characterisation and Antimicrobial Activity: An In-Vitro Study. *Cureus*. 2024 Jan 4;16(1):e51659. doi: 10.7759/cureus.51659. PMID: 38318582; PMCID: PMC10839412
- 28 Vani Raju M, Kaniyur Chandrasekaran M, Rajendran MS, Velliyur Kanniappan G, Muthaiyan Ahalliya R, Dugganaboyana GK, et al. Deciphering the Therapeutic, Larvicidal, and Chemical Pollutant Degrading Properties of Leaves-mediated Silver Nanoparticles Obtained from *Alpinia purpurata*. *BioRes* [Internet]. 2024 Apr. 12 [cited 2025 Sep. 3];19(2):3328-52. Available from: <https://ojs.bioresources.com/index.php/BRJ/article/view/23306>
29. Soni M, Pitchiah S, Suresh V, Ramasamy P, Sivaperumal P. Fabrication and partial characterization of silver nanoparticles from mangrove (*Avicennia marina*) leaves and their antibacterial efficacy against oral bacteria. *Cureus*. 2024 Jan 11;16(1).
30. Tharani M, Rajeshkumar S, Al-Ghanim KA, Nicoletti M, Sachivkina N, Govindarajan M. Terminalia chebula-assisted silver nanoparticles: biological potential, synthesis, characterization, and ecotoxicity. *Biomedicines*. 2023 May 18;11(5):1472.